Carbohydrate Polymers 112 (2014) 539–545

Contents lists available at ScienceDirect

Carbohydrate Polymers

journal homepage: www.elsevier.com/locate/carbpol

# Green synthesis of silver and gold nanoparticles employing levan, a biopolymer from *Acetobacter xylinum* NCIM 2526, as a reducing agent and capping agent

Khan Behlol Ayaz Ahmed [a], Divya Kalla [b], Kiran Babu Uppuluri [b,**], Veerappan Anbazhagan [a,*]

[a] Department of Chemistry, School of Chemical and Biotechnology, SASTRA University, Thanjavur, Tamil Nadu, India
[b] Department of Biotechnology, School of Chemical and Biotechnology, SASTRA University, Thanjavur, Tamil Nadu, India

ARTICLE INFO

*Article history:*
Received 8 May 2014
Received in revised form 5 June 2014
Accepted 13 June 2014
Available online 23 June 2014

*Keywords:*
Levan
*Acetobacter xylinum*
Silver nanoparticles
Gold nanoparticles
Catalyst

ABSTRACT

With a vision of finding greener materials to synthesize nanoparticles, we report the production and isolation of levan, a polysaccharide with repeating units of fructose, from *Acetobacter xylinum* NCIM2526. The isolated levan were characterized using potassium ferricyanide reducing power assay, Fourier transform infra-red (FTIR) spectroscopy and $^{1}$H nuclear magnetic resonance spectroscopy ($^{1}$H NMR). To exploit levan in nanotechnology, we present a simple and greener method to synthesize silver nanoparticles (AgNPs) and gold nanoparticles (AuNPs) using biopolymer, levan as both reducing and stabilizing agents. The morphology and stability of the AgNPs and AuNPs were examined by transmission electron microscopy (TEM) and UV–vis absorption (UV–vis) spectroscopy. The possible capping mechanism of the nanoparticles was postulated using FTIR studies. As synthesized biogenic nanoparticles showed excellent catalytic activity as evidenced from sodium borohydride mediated reduction of 4-nitro phenol and methylene blue.



## 1. Introduction

The growing awareness about the environment has forced the researchers to develop green methods to synthesize their desired product. The major requirements for any green synthesis are non-toxic chemicals, environmentally benign solvents and renewable materials. Nanostructures of noble metals particularly silver and gold nanostructures with 1–100 nm size has attracted significant interest over the years because of the unique size dependent optical, electrical and magnetic properties (Jain, Huang, El-Sayed, & El-Sayed, 2008; Li, Hu, Yang, & Alivisatos, 2001; Rao & Cheetham, 2001). Importantly those unique properties of nanostructures have been successfully utilized in various applications such as catalysis, optics, electronics, biotechnology, bioengineering, textile engineering, water treatment, silver based consumer products, biosensor and biological imaging (Evanoff & Chumanov, 2004; Haes et al., 2005; Hutter & Fendler, 2004; Mallick, Witcomb, & Scurrell, 2006; McFarland & Van Duyne, 2003; Nickel, Zu Castell, Pöppl, & Schneider, 2000). Because of such a wide range of applications, numerous methods including chemical, photochemical and biological methods have been developed to synthesize silver and gold nanostructures (Lu, Kobayashi, Tawa, & Ozaki, 2006; Sherry et al., 2005; Wiley et al., 2006). Among the synthetic methods, chemical reduction method is the most widely used one to prepare silver (AgNPs) and gold nanoparticles (AuNPs) with different size and morphology (Faramarzi & Sadighi, 2013). Typically, the preparation of metal nanoparticles involves the treatment of metal salts with a chemical reducing agent, such as sodium borohydride, hydrazine or other organic compounds in the presence of a suitable stabilizer (surfactants, polymers, tri block polymers and dendrimers) (Faramarzi & Sadighi, 2013; Guari et al., 2003; Koh, Ohno, Tsujii, & Fukuda, 2003; Mayya, Schoeler, & Caruso, 2003; Plyuto, Berquier, Jacquiod, & Ricolleau, 1999; Tan, Jiang, Li, & Zhu, 2002; Tanori & Pileni, 1997; Wang et al., 2002; Zhang et al., 2000). All these chemicals are highly reactive and associated with environmental and biological risks. Thus, there is a requirement to develop environmentally sustainable synthetic protocols to prepare stable metal NPs.

To prepare metal NPs by environmentally clean and sustainable way, researchers have begun to use biomolecules and bioorganism,

* Corresponding author. Tel.: +91 4362 264101x3689; fax: +91 4362 264120.
** Corresponding author. Tel.: +91 4362 264101x3635; fax: +91 4362 264120.
*E-mail addresses:* kiranbabu@scbt.sastra.edu (K.B. Uppuluri), anbazhagan@scbt.sastra.edu, anbugv@gmail.com (V. Anbazhagan).

http://dx.doi.org/10.1016/j.carbpol.2014.06.033
0144-8617/

such as bacteria, fungi, proteins, biopolymers and plant extracts (Ahmed, Subramanian, Sivasubramanian, Veerappan, & Veerappan, 2014; Narayanan & Sakthivel, 2010, 2011; Senapati, Ahmad, Khan, Sastry, & Kumar, 2005; Seralathan et al., 2014). Raveendran, Fu and Wallen (2003) reported the first preparation of AgNPs using the biopolymer, starch as a capping agent and D-glucose as the reducing agent. Of late, carbohydrates, such as glucose, sucrose, fructose, galactose, ribose and lactose are used as reducing agents (Valodkar, Bhadoria, Pohnerkar, Mohan, & Thakore, 2010) and biopolymers such as starch, cellulose, chitosan, pectin and guar gum are used as capping agents (Fanta, Kenar, Felker, & Byars, 2013; George et al., 2014; Lavorgna et al., 2014; Raghavendra, Jayaramudu, Varaprasad, Sadiku, Ray, & Mohana Raju, 2013; Venkatakrishnan, Veerappan, Elamparuthi, & Veerappan, 2014). Biopolymers can stabilize nanoparticles *via* electrostatic interaction of their functional groups with the nanoparticles and are believed to be excellent host systems for metal nanoparticles.

Levan, a homo polysaccharide derived from plants and microorganisms, composed of fructofuranosyl residues linked by $\beta$-(2,6)-glycosidic linkage and is widely used in many different fields, including medicine, food and beverage industry, cosmetics and pharmaceuticals (Abdel-Fattah, Gamal-Eldeen, Helmy, & Esawy, 2012; Han, 1990; Jang et al., 2001; Kang et al., 2009; Shih, Yu, Shieh, & Hsieh, 2005; Zhang et al., 2014). In addition, derivatives of levan are potential anti-AIDS agent. It is completely degraded by the gut microflora and exhibit prebiotic and hypocholesterolaemic effects (Yamamoto et al., 1999). Levan is an attractive and promising biopolymer for nanotechnology, because of their benign nature and contains higher number of hydroxyl and reducing keto sugar unit. Since levan possesses many properties favorable and beneficial for human health, an attempt was made to produce levan using Gram-negative bacterium *Acetobacter xylinum* (*A. xylinum*) NCIM 2526. *A. xylinum* is an interesting bacterium, which is able to synthesize two different exopolysaccharides; either levan or cellulose, just by changing the carbon source of the medium (Tajima et al., 1997). In this work, we produced levan by growing *A. xylinum* on a sucrose medium. The obtained levan was analyzed by potassium ferricyanide ($K_3[Fe(CN)_6]$) reducing power assay (PFA) (Brushwood, 2000), Fourier transform infra-red (FTIR) and $^1$H nuclear magnetic resonance spectroscopy ($^1$H NMR) spectroscopy. To exploit levan in nanotechnology, we present a simple and green method for the preparation of silver and gold nanoparticles using levan as both the reducing and stabilizing agents. This is also the first report on the preparation of AgNPs and AuNPs by reduction of the corresponding metal salts using polysaccharide levan. The resulting AgNPs and AuNPs were stable and characterized by UV–vis absorption spectroscopy (UV–vis), transmission electron microscopy (TEM) and FTIR. To extend the application of levan stabilized AgNPs and AuNPs, we investigated the catalytic activity of the NPs using standard reaction: reduction of 4-nitro phenol (4-NP) and methylene blue (MB). The details of the investigation are reported below.

## 2. Materials and methods

### 2.1. Materials

*A. xylinum* NCIM 2526 strain was obtained from NCL, Pune, India. Luria broth was purchased from Himedia Chemicals India Pvt. Ltd (Mumbai, India). Silver nitrate, ethanol, sucrose, peptone, ammonium sulphate, potassium dihydrogen phosphate, magnesium sulphate heptahydrate, potassium ferricyanide, potassium hydroxide, calcium chloride, sodium hydroxide and sodium borohydride were purchased from Merck, India. Gold chloride ($AuCl_3$) was obtained from Alfa Aesar, India. Millipore water with a resistivity more than 18.0 MΩ was used for the preparation of all aqueous solutions. All the glasswares were cleaned with freshly prepared aqua regia (3:1, HCl: $HNO_3$) and rinsed thoroughly with water. Then they were dry sterilized using hot air oven at 160 °C for 3 h, prior to use.

### 2.2. Production and isolation of levan

*A. xylinum* was cultured in Luria-broth liquid medium (6% sucrose, 1.5% peptone, 0.2% ammonium sulphate, 0.1% potassium dihydrogen phosphate, 0.1% magnesium sulphate heptahydrate, pH 6.8) at 28 °C for the production of levan. After 36 h incubation, the exopolysaccharide, levan was harvested in the broth. To remove the dissolved protein, the broth was heated to boil at 100 °C. After cooling, the broth was centrifuged for 30 min at 8000 rpm. The resultant supernatant was further boiled for 5 min to deactivate any residual extracellular enzymes. After cooling down to room temperature, the pH of the supernatant was adjusted to 10 by using 1 M KOH. Then, twice the amount of 80% cold ethanol was added. Levan was precipitated by the addition of 1% calcium chloride (1 ml per 10 mL supernatant–ethanol solution) under rigorous stirring for 20 min. The precipitate was collected by centrifugation for 15 min at 13,000 rpm. The resultant pellet was washed with 1.5 volumes of 80% cold ethanol and freeze dried. The presence of fructose in the isolated levan was judged by PFA. Briefly, 1 mL of $K_3[Fe(CN)_6]$ (10 mg/mL, dissolved in 20% sodium hydroxide aqueous solution) was added to the test tube containing 1 mg/mL of hydrolyzed levan. The content was gently shaken and color change was closely monitored. As a control samples, we used glucose and fructose. The disappearance of the greenish yellow color indicates the presence of reducing sugar. The functional group present in the polysaccharide was identified by FTIR spectroscopy. FTIR spectroscopic measurements were carried out on a Perkin Elmer spectrum-one instrument in the diffuse reflectance mode at a resolution of 1 $cm^{-1}$ in KBr pellet. $^1$H NMR was measured in a Bruker 300 MHz instrument.

### 2.3. Preparation of silver and gold nanoparticles

Typically, 20 mg of levan was dissolved in 49 mL of 0.2% sodium hydroxide solution. A 1 mL of silver nitrate (1 mM final concentration) aqueous solution was added to the alkaline levan solution. The mixture solution was allowed to stir at room temperature for 5 min and then heated to 100 °C. The appearance of brown color indicated the reduction of silver ion into AgNPs. In parallel, AgNPs were prepared by chemical reduction method. Briefly, 20 mg of levan was dissolved in 49 mL of 0.04% sodium hydroxide solution. To the biopolymeric solution, 1 mL of aqueous $AgNO_3$ (1 mM final concentration) was added slowly under vigorous stirring. After 5 min, 0.2 mM $NaBH_4$ was added as a reducing agent. The immediate appearance of brown color indicated the formation of AgNPs.

Gold nanoparticles were prepared by heating (100 °C) 1 mM gold chloride in alkaline levan solution for 30 min. The appearance of purple color indicates the formation of AuNPs. Similarly, AuNPs were prepared by chemical reduction method using levan as a capping agent. Briefly, addition of 6 mM $NaBH_4$ to 1 mM $AuCl_3$ solution produced dark purple color, indicating the reduction of $Au^{3+}$ to $Au^0$. All reactions were repeated at least three times to confirm the reproducibility of nanoparticles formation. The synthesized NPs characterization was carried out after allowing the solution to stand at room temperature for more than one week.

### 2.4. Characterization of levan stabilized nanoparticles

UV–vis was performed on a Thermo Scientific Evolution 201 spectrophotometer operated at 1 nm resolution. The size and

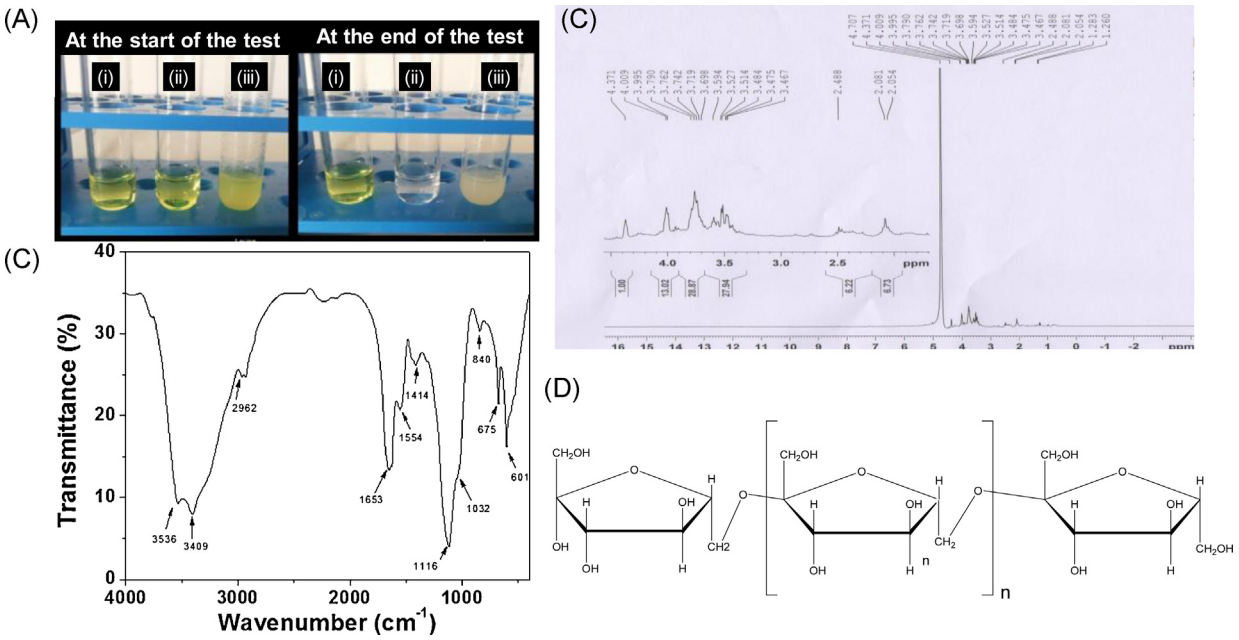


**Fig. 1.** Characterization of *A. xylinum* levan (A) potassium ferricyanide reducing power assay (i) glucose (1 mg/mL), (ii) fructose (1 mg/ml) and (iii) hydrolyzed levan (B) FTIR spectra, (C) $^1$H NMR spectra and (D) Structure of levan.

morphology were examined using high-resolution transmission electron microscopy (HR-TEM) (JEOL-JEM 1011, Japan) operating at an accelerated voltage of 200 kV. The samples were prepared by placing a drop of NPs solution on a graphite grid and drying it in vacuum.

### 2.5. Catalytic application of levan stabilized nanoparticles

The catalytic ability of AgNPs and AuNPs was evaluated using the standard reduction reaction. Briefly, an aliquot of 4-NP solution (0.05 mM in water) was treated with sodium borohydride ($NaBH_4$) solution (35 mM) and its absorbance was measured at 401 nm. The addition of NPs (100 μL of 1 mM stock) to the 4-NP solution produced a color change from yellowish-green to colorless. A new peak appeared at 301 nm with concomitant disappearance of the peak at 401 nm within 1 min indicating the complete reduction of 4-NP to 4-aminophenol (4-AP).

Similarly, addition of AgNPs or AuNPs (100 μL of 1 mM stock) and $NaBH_4$ (32 mM) into the MB aqueous solution at room temperature produced a color change from blue to colorless. The disappearance of the methylene blue absorption peak at 664 nm happened in few seconds, indicating the complete reduction of methylene blue.

## 3. Results and discussion

Because of the commercial values, the research on the production of levan has been intensified (Zhang et al., 2014) in the recent years. In this paper, we demonstrate the production of levan using *A. xylinum* culture aerobically by incubating for 36 h as described in the materials and methods. The obtained polysaccharide was characterized using PFA, $^1$H NMR and FTIR. PFA is a very useful method to distinguish fructose from other monosaccharides, like glucose and galactose (Brushwood, 2000). The addition of alkaline $K_3[Fe(CN)_6]$ to 1 mg/mL of levan produced greenish yellow color solution. As a control, we added alkaline $K_3[Fe(CN)_6]$ to fructose and glucose. The greenish yellow color of the levan and fructose disappeared within 2 min, whereas, for glucose it took about 8 min (Fig. 1A). These results suggest that the polysaccharide isolated from *A. xylinum* species would constitute the repeating unit of fructose. FTIR spectra (KBr pellet) of the purified levan (Fig. 1B) show an absorption band due to the carbonyl stretching (C=O) at 1638 $cm^{-1}$. The O—H stretching is seen at 3409 and 3545 $cm^{-1}$. The C—H stretching vibration is seen at 2962 $cm^{-1}$, C—H bending is seen at 1414 $cm^{-1}$. The absorption band at 1032 and 1116 $cm^{-1}$ indicates the pyranose form of sugars. The region in the range of 900–1200 $cm^{-1}$ corresponds to the finger print region of the molecule, which is dominated by ring vibrations overlapped with stretching vibration of (C—OH) side groups and the (C—O—C) glycosidic bond vibration. The obtained FTIR pattern of *A. xylinum* levan is consistent with the reference levan according to Barone and Medynets (2007). $^1$H NMR spectra show proton peak between 3.4 and 4.3 (Fig. 1C), indicating the presence of sugar protons, which are almost identical with peak positions for levan produced by *Bacillus subtilis* and *Pseudomonas fluorescens* (Han, 1990; Shih et al., 2005). The structure of the levan is shown in Fig. 1D.

Levan has been used as an encapsulating agent, emulsifier and surface-finishing agent in the food industry. But, there are no reports so far on the utilization of levan in producing nanomaterials. The growing demand for biocompatible capping agent to prevent nanoparticles agglomeration encouraged us to develop a new method to synthesize biogenic AgNPs and AuNPs using levan. Addition of 1 mM solution of $AgNO_3$ into the alkaline solution of levan did not produce any significant color change and only resulted in the formation of turbid pale-brown color solution (Fig. 2). UV–vis does not show the characteristic surface plasmon resonance (SPR) peak of AgNPs. The turbid solution was stable for more than five days in the ambient condition. It is also noted that levan solution did not show any absorption in the visible range. However, upon heating the mixture at 100 °C, the turbid levan-$AgNO_3$ solution immediately turned into dark brown color, which confirms the formation of AgNPs. The absorption studies revealed a broad SPR absorption peak with $\lambda_{max}$ at 406 nm along with a shoulder at 540 nm. It is a well-known phenomenon that the position and shape of the AgNPs SPR peak depends on the particle size, shape and dielectric constant of the surrounding medium (Kelly, Coronado, Zhao, & Schatz, 2003). The obtained broad SPR band is indicative of polydispersed NPs formation in the aqueous solution. Instead

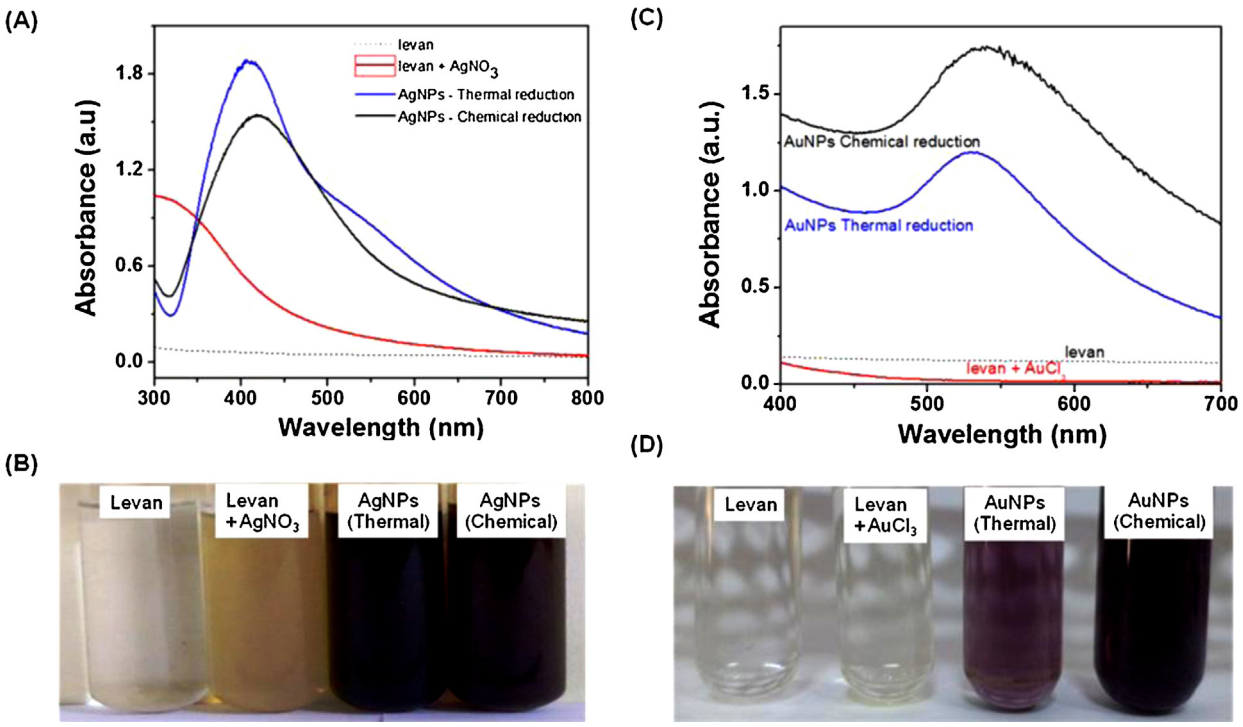


**Fig. 2.** Absorption spectra of the metal NPs prepared by thermal and chemical reduction methods. (A) UV–vis spectra of AgNPs, (B) AgNPs digital photograph corresponding to the absorption spectra (A), (C) UV–vis spectra of AuNPs and (D) AuNPs digital photograph corresponding to the absorption spectra (C).

of heating, addition of $NaBH_4$ to the levan-$AgNO_3$ produced dark brown solution suggesting the formation of AgNPs. The absorption spectrum of AgNPs prepared by this method shows a single SPR peak with center at 418 nm (Fig. 2A). The complete elimination of the peak at 540 nm presumably indicates the change in the polydispersity of the NPs. It was found that the color and UV–vis absorption peak of the levan stabilized AgNPs does not change even after a month, indicating the presence of well dispersed stable nanoparticles in the solution.

At room temperature, alkaline levan solution did not have the ability to reduce $AuCl_3$ to AuNPs. However, on heating $AuCl_3$ aqueous solution in the presence of levan produced a purple color solution, suggesting the conversion of $Au^{3+}$ to $Au^0$. The UV–vis absorption spectra recorded from the resulting solutions show the characteristic SPR band of AuNPs centered at about 530 nm (Fig. 1) (Ahmed et al., 2014). AuNPs prepared with chemical reduction method show a broad peak with a maximum at 539 nm. The dispersity of AuNPs prepared by thermal and chemical reduction method was evaluated by comparing the full width at half-maximum (FWHM) from the UV–vis spectra (Janani, Stevenson, & Veerappan, 2014; Wilcoxon & Abrams, 2006). The FWHM calculated for AuNPs synthesized by thermal reduction is 60 nm, whereas FWHM is 89 nm for the AuNPs prepared by chemical reduction method. These results suggest that the chemical reduction method produces relatively polydispersed AuNPs.

Typical TEM images of AgNPs and AuNPs obtained with levan are shown in Fig. 3. The observed fringes pattern in HR-TEM supports the crystalline nature of the as-prepared AgNPs and AuNPs (inset in Fig. 3). Both thermal and chemical reduction method produces spherical nanoparticles. The AgNPs prepared by heating show polydispersed nanoparticles with size distribution range from 10 to 29 nm (Fig. 3A). However, AgNPs prepared by chemical reduction method show narrow size distribution range from 5 to 8 nm (Fig. 3B), augmenting the observed UV–vis spectral characteristics of the AgNPs. On contrary, AuNPs prepared by thermal reduction method show narrow size distribution range from 10 to 12 nm (Fig. 3C); whereas, chemical reduction method show polydispersed NPs with size distribution range from 10 to 30 nm (Fig. 3D) supporting the UV–vis spectral measurements (Fig. 2C).

To determine the interaction between levan and NPs, FTIR spectra of levan and levan stabilized AgNPs are compared (Fig. 4). IR peaks at 1650 $cm^{-1}$ and 3400 $cm^{-1}$, which are characteristics of carbonyl and hydroxyl groups, respectively, are present in both levan and the levan stabilized AgNPs spectra (Fig. 4A), indicating the presence of levan around the particles. The broad band at 3400 $cm^{-1}$ is attributed to a possible intermolecular hydrogen-bonded network of O—H of the levan on the surface of the nanoparticles. Noteworthy, the finger print region (1200–900 $cm^{-1}$) corresponding to stretching vibration of (C—OH) side groups and the (C—O—C) glycosidic bond is shifted due to the possible interaction between metal nanoparticles and levan (Fig. 4B). It is clear from HR-TEM images that the formed nanoparticles are isotropic (i.e., low aspect ratio) in shape. These results support the formation of AgNPs inside the nanoscopic polysaccharide templates. Thus, we propose that the electrostatic attractive forces between levan, hydroxyl group and silver ion in solution provide an effective driving force for the formation and stabilization of the AgNPs.

In order to explore the levan stabilized AgNPs and AuNPs in nanotechnology applications; we evaluated the catalytic activity of the AgNPs and AuNPs using two standard model reactions: the reduction of 4-NP and MB by sodium borohydride ($NaBH_4$). The chosen reaction was easy to follow by UV–vis absorption spectroscopy. Therefore, this reaction has been used widely to evaluate the catalytic activity of various metallic NPs including silver, gold, copper, nickel, palladium and platinum (Ahmed et al., 2014; Venkatakrishnan et al., 2014). The addition of $NaBH_4$ to the aqueous solution of 4-NP was accompanied by a color change from light yellow to yellowish-green (Fig. 5A), indicating the formation 4-nitrophenolate ion. The addition of 100 μL of levan stabilized NPs to 4-nitrophenolate ion gradually diminished the yellow color of the reaction mixture in a time dependent manner, suggesting the reduction of 4-NP to 4-AP (Fig. 5A). The disappearance of an

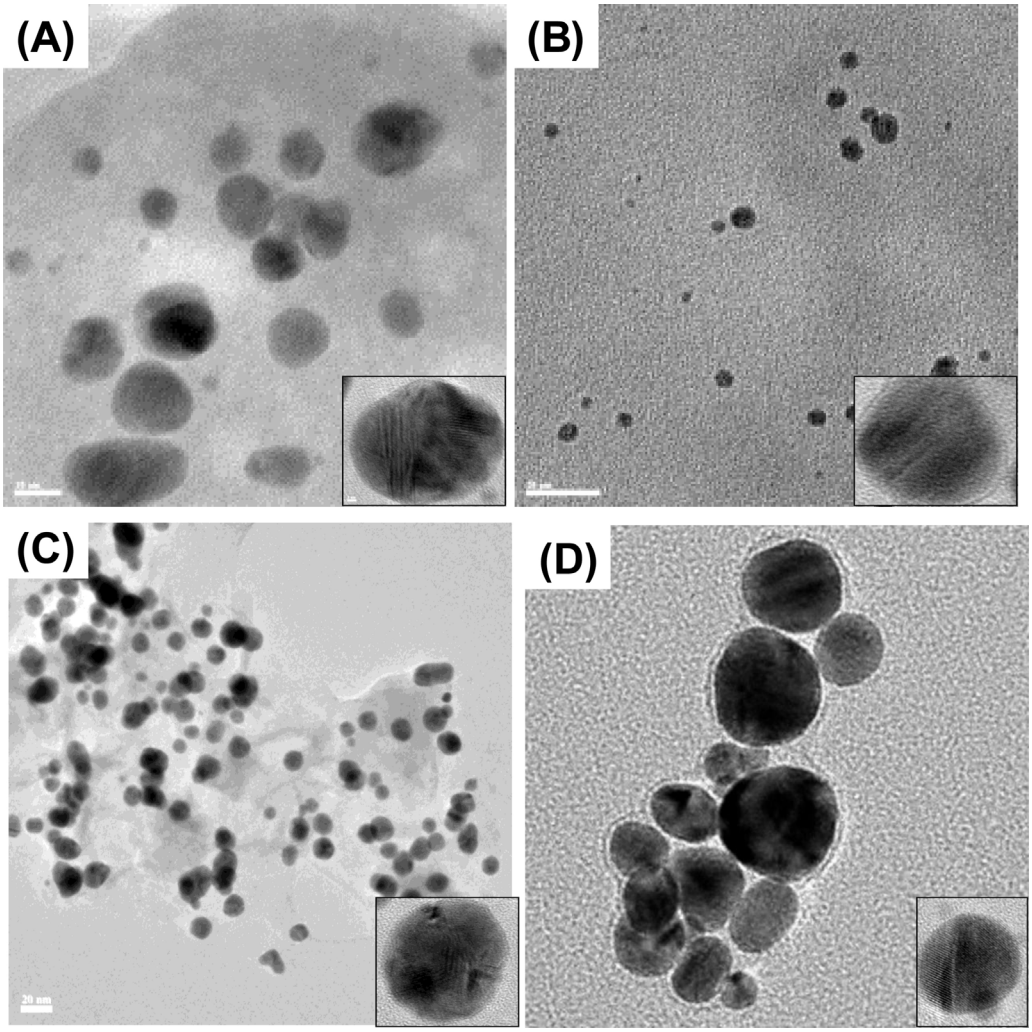


**Fig. 3.** TEM image of levan stabilized AgNPs (A), (B) and AuNPs (C), (D). *Inset* corresponds to the HR-TEM image. (A) and (C) correspond to the respective NPs prepared by thermal reduction method and, (B) and (D) correspond to the respective NPs prepared by chemical reduction method.

absorption peak at 401 nm and the appearance of a new peak at 301 nm clearly confirms the formation of 4-AP (Fig. 5B).

The addition of NPs and $NaBH_4$ immediately diminishes the blue color of MB to a colorless solution (Fig. 6A). In aqueous medium, MB shows an absorption maximum at 664 nm accompanied with a shoulder at 614 nm (Fig. 6B). The disappearance of MB absorption peak clearly indicates the reduction of MB to its Leuco form (Fig. 6B) (Ahmed et al., 2014). As noted, the addition of $NaBH_4$ to MB aqueous solution in the absence of nanoparticle at room temperature decreases the absorption maximum at a very slow rate (Fig. 6B). However, addition of small quantity of NPs greatly enhanced the decay process. Since the bleaching of 4-NP and MB color is very rapid, it was difficult to estimate the exact reduction rate using the conventional UV–vis spectrophotometer. Nevertheless, our study

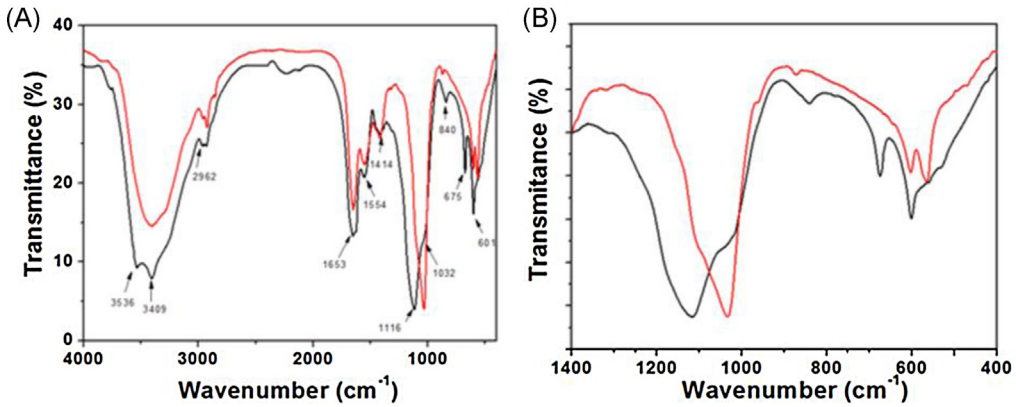


**Fig. 4.** (A) Comparative FTIR spectra of levan (black line) and levan capped AgNPs (red line). (B) FTIR spectra of the finger print region. (For interpretation of the references to color in text, the reader is referred to the web version of this article.)

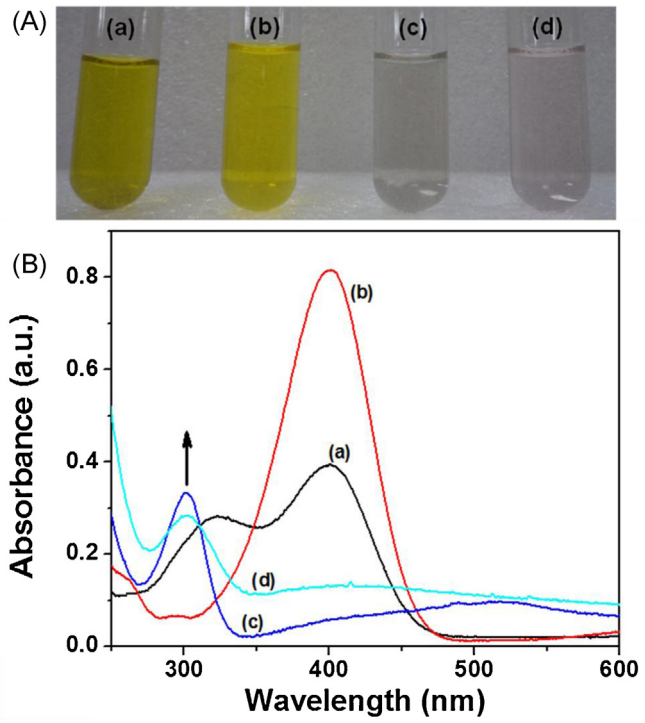


**Fig. 5.** (A) Digital image of the conversion of 4-NP to 4-AP: (a) 4-NP, (b) 4-nitrophenolate ion, (c) AgNPs mediated reduced product, 4-AP, (d) AuNPs mediated reduced product, 4-AP. (B) Corresponding UV–vis spectra of the digital image (A). Levan stabilized AgNPs/AuNPs act as catalyst and $NaBH_4$ act as a reducing agent. Arrow indicates new absorption peak, characteristics of 4-AP.

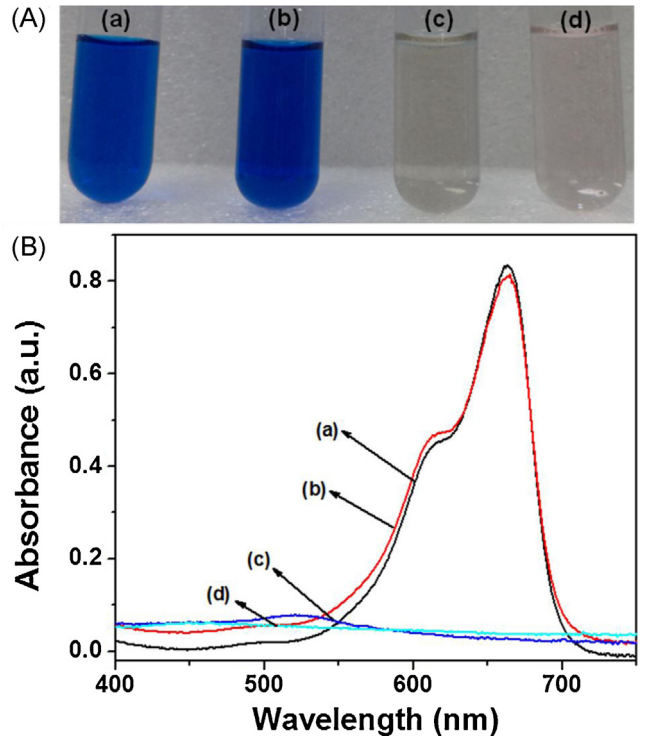


**Fig. 6.** (A) Digital image of the conversion of methylene blue (MB) to leucomethylene blue (leuco-MB): (a) MB, (b) MB, after 10 min addition of $NaBH_4$, (c) AgNPs mediated reduced product, leuco-MB, (d) AuNPs mediated reduced product, leuco-MB. (B) Corresponding UV–vis spectra of the digital image (A). Levan stabilized AgNPs/AuNPs act as catalyst and $NaBH_4$ act as a reducing agent.

clearly indicates that the levan stabilized AgNPs and AuNPs have an inherent potential to act as a catalyst.

## 4. Conclusion

In this work, we report the production and isolation of biopolymer, levan using *A. xylinum*. To the best of our knowledge, this is the first report showing the potential of levan in synthesizing inorganic nanoparticles. FTIR and UV–vis spectroscopic studies indicate the capping of the nanoparticles with levan. The NPs produced are highly stable and show no signs of aggregation even after two months of storage. The reported method to prepare optically active AgNPs and AuNPs is greener and biocompatible. Moreover, the widespread occurrence of levan makes this process amenable to large scale industrial production. The synthesized AgNPs and AuNPs have great potential to act as catalyst, as evidenced from the reduction of 4-nitro phenol and methylene blue. Studies with different organic substrates are in progress to extend the catalytic activity of the green synthesized AgNPs and AuNPs.

## Acknowledgements

KBAA earnestly acknowledge the teaching assistantship from SASTRA University, Thanjavur, India. VA (SB/FT/LS-217/2012) and KB thank Department of Science, India for the funding. We thank Central Research Facility, SASTRA University for providing the necessary infrastructure.

## References

Abdel-Fattah, A. M., Gamal-Eldeen, A. M., Helmy, W. A., & Esawy, M. A. (2012). Antitumor and antioxidant activities of levan and its derivative from the isolate *Bacillus subtilis* NRC1aza. *Carbohydrate Polymers*, *89*(2), 314–322.

Ahmed, K. B. A., Subramanian, S., Sivasubramanian, A., Veerappan, G., & Veerappan, A. (2014). Preparation of gold nanoparticles using *Salicornia brachiata* plant extract and evaluation of catalytic and antibacterial activity. *Spectrochimica Acta, Part A: Molecular and Biomolecular Spectroscopy*, *130*, 54–58.

Barone, J. R., & Medynets, M. (2007). Thermally processed levan polymers. *Carbohydrate Polymers*, *69*(3), 554–561.

Brushwood, D. E. (2000). Modification of the potassium ferricyanide reducing sugar test for sugars from extracts of cotton fiber. *Journal of Cotton Science*, *4*(3), 202–209.

Evanoff, D. D., & Chumanov, G. (2004). Size-controlled synthesis of nanoparticles: 1.Silver-only aqueous suspensions via hydrogen reduction. *Journal of Physical Chemistry B*, *108*(37), 13948–13956.

Fanta, G. F., Kenar, J. A., Felker, F. C., & Byars, J. A. (2013). Preparation of starch-stabilized silver nanoparticles from amylose–sodium palmitate inclusion complexes. *Carbohydrate Polymers*, *92*(1), 260–268.

Faramarzi, M. A., & Sadighi, A. (2013). Insights into biogenic and chemical production of inorganic nanomaterials and nanostructures. *Advances in Colloid and Interface Science*, *189*, 1–20.

George, J., Kumar, R., Sajeevkumar, V. A., Ramana, K. V., Rajamanickam, R., Abhishek, V., et al. (2014). Hybrid HPMC nanocomposites containing bacterial cellulose nanocrystals and silver nanoparticles. *Carbohydrate Polymers*, *150*, 285–292.

Guari, Y., Thieuleux, C., Mehdi, A., Reyé, C., Corriu, R. J., Gomez-Gallardo, S., et al. (2003). In situ formation of gold nanoparticles within thiol functionalized HMS-C16 and SBA-15 type materials via an organometallic two-step approach. *Chemistry of Materials*, *15*(10), 2017–2024.

Haes, A. J., Haynes, C. L., McFarland, A. D., Schatz, G. C., Van Duyne, R. P., & Zou, S. (2005). Plasmonic materials for surface-enhanced sensing and spectroscopy. *MRS Bulletin*, *30*(05), 368–375.

Han, Y. W. (1990). Microbial levan. *Advances in Applied Microbiology*, *35*, 171–194.

Hutter, E., & Fendler, J. H. (2004). Exploitation of localized surface plasmon resonance. *Advanced Materials*, *16*(19), 1685–1706.

Jain, P. K., Huang, X., El-Sayed, I. H., & El-Sayed, M. A. (2008). Noble metals on the nanoscale: Optical and photothermal properties and some applications in imaging, sensing, biology, and medicine. *Accounts of Chemical Research*, *41*(12), 1578–1586.

Janani, S., Stevenson, P., & Veerappan, A. (2014). Activity of catalytic silver nanoparticles modulated by capping agent hydrophobicity. *Colloids and Surfaces B: Biointerfaces*, http://dx.doi.org/10.1016/j.colsurfb.2014.03.008

Jang, K.-H., Song, K.-B., Kim, C. H., Chung, B. H., Kang, S. A., Chun, U.-H., et al. (2001). Comparison of characteristics of levan produced by different preparations of levansucrase from *Zymomonas mobilis*. *Biotechnology Letters*, *23*(5), 339–344.

Kang, S. A., Jang, K.-H., Seo, J.-W., Kim, K. H., Kim, Y. H., Rairakhwada, D., et al. (2009). Levan: applications and perspectives. In *Microbial production of biopolymers and polymer precursors*. Norwich: Caister Academic Press.

Kelly, K. L., Coronado, E., Zhao, L. L., & Schatz, G. C. (2003). The optical properties of metal nanoparticles: The influence of size, shape, and dielectric environment. *Journal of Physical Chemistry B*, *107*(3), 668–677.

Koh, K., Ohno, K., Tsujii, Y., & Fukuda, T. (2003). Precision synthesis of organic/inorganic hybrid nanocapsules with a silanol-functionalized micelle template. *Angewandte Chemie*, *115*(35), 4326–4329.

Lavorgna, M., Attianese, I., Buonocore, G., Conte, A., Del Nobile, M., Tescione, F., et al. (2014). MMT-supported Ag nanoparticles for chitosan nanocomposites: Structural properties and antibacterial activity. *Carbohydrate Polymers*, *102*, 385–392.

Li, L.-S., Hu, J., Yang, W., & Alivisatos, A. P. (2001). Band gap variation of size-and shape-controlled colloidal CdSe quantum rods. *Nano Letters*, *1*(7), 349–351.

Lu, L., Kobayashi, A., Tawa, K., & Ozaki, Y. (2006). Silver nanoplates with special shapes: Controlled synthesis and their surface plasmon resonance and surface-enhanced Raman scattering properties. *Chemistry of Materials*, *18*(20), 4894–4901.

Mallick, K., Witcomb, M., & Scurrell, M. (2006). Silver nanoparticle catalysed redox reaction: An electron relay effect. *Materials Chemistry and Physics*, *97*(2), 283–287.

Mayya, K. S., Schoeler, B., & Caruso, F. (2003). Preparation and organization of nanoscale polyelectrolyte-coated gold nanoparticles. *Advanced Functional Materials*, *13*(3), 183–188.

McFarland, A. D., & Van Duyne, R. P. (2003). Single silver nanoparticles as real-time optical sensors with zeptomole sensitivity. *Nano Letters*, *3*(8), 1057–1062.

Narayanan, K. B., & Sakthivel, N. (2010). Biological synthesis of metal nanoparticles by microbes. *Advances in Colloid and Interface Science*, *156*(1), 1–13.

Narayanan, K. B., & Sakthivel, N. (2011). Green synthesis of biogenic metal nanoparticles by terrestrial and aquatic phototrophic and heterotrophic eukaryotes and biocompatible agents. *Advances in Colloid and Interface Science*, *169*(2), 59–79.

Nickel, U., Zu Castell, A., Pöppl, K., & Schneider, S. (2000). A silver colloid produced by reduction with hydrazine as support for highly sensitive surface-enhanced Raman spectroscopy. *Langmuir*, *16*(23), 9087–9091.

Plyuto, Y., Berquier, J.-M., Jacquiod, C., & Ricolleau, C. (1999). Ag nanoparticles synthesised in template-structured mesoporous silica films on a glass substrate. *Chemical Communications*, *17*, 1653–1654.

Raghavendra, G. M., Jayaramudu, T., Varaprasad, K., Sadiku, R., Ray, S. S., & Mohana Raju, K. (2013). Cellulose–polymer–Ag nanocomposite fibers for antibacterial fabrics/skin scaffolds. *Carbohydrate Polymers*, *93*(2), 553–560.

Rao, C., & Cheetham, A. (2001). Science and technology of nanomaterials: Current status and future prospects. *Journal of Materials Chemistry*, *11*(12), 2887–2894.

Raveendran, P., Fu, J., & Wallen, S. L. (2003). Completely green synthesis and stabilization of metal nanoparticles. *Journal of the American Chemical Society*, *125*(46), 13940–13941.

Senapati, S., Ahmad, A., Khan, M. I., Sastry, M., & Kumar, R. (2005). Extracellular biosynthesis of bimetallic Au–Ag alloy nanoparticles. *Small*, *1*(5), 517–520.

Seralathan, J., Stevenson, P., Subramaniam, S., Raghavan, R., Pemaiah, B., Sivasubramanian, A., et al. (2014). Spectroscopy investigation on chemo-catalytic, free radical scavenging and bactericidal properties of biogenic silver nanoparticles synthesized using Salicornia brachiata aqueous extract. *Spectrochimica Acta, Part A: Molecular and Biomolecular Spectroscopy*, *118*, 349–355.

Sherry, L. J., Chang, S.-H., Schatz, G. C., Van Duyne, R. P., Wiley, B. J., & Xia, Y. (2005). Localized surface plasmon resonance spectroscopy of single silver nanocubes. *Nano Letters*, *5*(10), 2034–2038.

Shih, I.-L., Yu, Y.-T., Shieh, C.-J., & Hsieh, C.-Y. (2005). Selective production and characterization of levan by *Bacillus subtilis* (Natto) Takahashi. *Journal of Agricultural and Food Chemistry*, *53*(21), 8211–8215.

Tajima, K., Uenishi, N., Fujiwara, M., Erata, T., Munekata, M., & Takai, M. (1997). The production of a new water-soluble polysaccharide by *Acetobacter xylinum* NCI 1005 and its structural analysis by NMR spectroscopy. *Carbohydrate Research*, *305*(1), 117–122.

Tan, Y., Jiang, L., Li, Y., & Zhu, D. (2002). One dimensional aggregates of silver nanoparticles induced by the stabilizer 2-mercaptobenzimidazole. *Journal of Physical Chemistry B*, *106*(12), 3131–3138.

Tanori, J., & Pileni, M. (1997). Control of the shape of copper metallic particles by using a colloidal system as template. *Langmuir*, *13*(4), 639–646.

Valodkar, M., Bhadoria, A., Pohnerkar, J., Mohan, M., & Thakore, S. (2010). Morphology and antibacterial activity of carbohydrate-stabilized silver nanoparticles. *Carbohydrate Research*, *345*(12), 1767–1773.

Venkatakrishnan, S., Veerappan, G., Elamparuthi, E., & Veerappan, A. (2014). Aerobic synthesis of biocompatible copper nanoparticles: Promising antibacterial agent and catalyst for nitroaromatic reduction and C—N cross coupling reaction. *RSC Advances*, *4*(29), 15003–15006.

Wang, T., Zhang, D., Xu, W., Yang, J., Han, R., & Zhu, D. (2002). Preparation, characterization, and photophysical properties of alkanethiols with pyrene units-capped gold nanoparticles: Unusual fluorescence enhancement for the aged solutions of these gold nanoparticles. *Langmuir*, *18*(5), 1840–1848.

Wilcoxon, J., & Abrams, B. (2006). Synthesis, structure and properties of metal nanoclusters. *Chemical Society Reviews*, *35*(11), 1162–1194.

Wiley, B. J., Im, S. H., Li, Z.-Y., McLellan, J., Siekkinen, A., & Xia, Y. (2006). Maneuvering the surface plasmon resonance of silver nanostructures through shape-controlled synthesis. *Journal of Physical Chemistry B*, *110*(32), 15666–15675.

Yamamoto, Y., Takahashi, Y., Kawano, M., Iizuka, M., Matsumoto, T., Saeki, S., et al. (1999). In vitro digestibility and fermentability of levan and its hypocholesterolemic effects in rats. *Journal of Nutritional Biochemistry*, *10*(1), 13–18.

Zhang, Z., Patel, R. C., Kothari, R., Johnson, C. P., Friberg, S. E., & Aikens, P. A. (2000). Stable silver clusters and nanoparticles prepared in polyacrylate and inverse micellar solutions. *Journal of Physical Chemistry B*, *104*(6), 1176–1182.

Zhang, T., Li, R., Qian, H., Mu, W., Miao, M., & Jiang, B. (2014). Biosynthesis of levan by levansucrase from *Bacillus methylotrophicus* SK 21.002. *Carbohydrate Polymers*, *101*, 975–981.